

Halos and voids in a multifractal model of cosmic structure

José Gaite

Instituto de Matemáticas y Física Fundamental, CSIC, Serrano 113bis, 28006 Madrid, Spain

29 November 2006

ABSTRACT

On the one hand, the large scale structure of matter is arguably scale invariant, and, on the other hand, halos and voids are recognized as prominent features of that structure. To unify both approaches, we propose to model the dark matter distribution as a set of fractal distributions of halos of different kinds. This model relies on the concept of multifractal as the most general scaling distribution and on a plausible notion of halo as a *singular* mass concentration in a multifractal. Voids arise as complementary to halos, namely, as formed by *regular* mass depletions. To provide halos with definite size and masses, we coarse-grain the dark matter distribution using a natural length derived from the lower scaling limit. This allows us to relate the *halo mass function* to the *multifractal spectrum*. Hence, we find that a log-normal model of the mass distribution nicely fits in this picture and, moreover, the Press-Schechter mass function can be recovered as a *bifractal* limit.

To support our model of fractal distributions of halos, we perform a numerical study of the distribution produced in cosmological N -body simulations. In the Virgo Λ -CDM GIF2 simulation, we indeed find fractal distributions of halos with various dimensions and a halo mass function of bifractal type. However, this mass function is just beyond the Press-Schechter's range, and we interpret it instead as caused by the *undersampling* of the distribution at the scale of halos, due to discretization.

Subject headings: cosmology: large-scale structure of the universe – galaxies: clusters: general – methods: statistical

1. Introduction

Current research on the large scale structure of matter is concerned with two fundamental concepts: halo and void. The concept of halo applies to the dark matter distribution and is meant to define the basic unit of structure. Therefore, dark matter halos have theoretical rather than observational basis. In particular, the concept of halo is useful in the analysis of N -body cosmological simulations. In contrast, the concept of void arose in observations of the galaxy distribution, although, recently, it has also been applied to the dark matter distribution and gained some theoretical basis.

On a more fundamental level, the principle of scale invariance has been often applied to the study of the large scale structure of matter. Scale invariance is a general symmetry, with applica-

tions in various branches of physics and other sciences. Its application in cosmology is old, dating back to hierarchical models of the Universe devised before the discovery of General Relativity (Mandelbrot, 1977). It became part of standard cosmology when the analysis of galaxy catalogues proved that the two-point correlation function is a power law on scales of several Mpc. A recent review of various ideas and models in cosmology based on scaling laws is given by Jones et al (2004). Of particular importance are fractal models (Sylos Labini, Montuori & Pietronero, 1998). Multifractal models (Parisi & Frisch, 1985; Halsey et al, 1986) are an improvement of fractal models and were introduced in cosmology by Pietronero (1987), Jones et al (1988) and Balian & Schaeffer (1988). Multifractal analyses of large-scale structure were initially applied to the distribu-

tion of galaxies (Domínguez-Tenreiro & Martínez, 1989; Martínez, Jones, Domínguez-Tenreiro & van de Weygaert, 1990) and later applied to N -body simulations (Colombi, Bouchet & Schaeffer, 1992; Valdarnini, Borgani & Provenzale, 1992; Yepes, Domínguez-Tenreiro & Couchman, 1992).

We shall take scale invariance of the dark matter distribution in the *nonlinear* regime as our working hypothesis. This hypothesis leads essentially to a multifractal model (with transition to homogeneity). Since the linear regime departs from the initial scale invariance (Harrison-Zeldovich spectrum), the initial conditions for nonlinear evolution are not scale invariant. However, the dynamical equations for cold dark matter are scale invariant. Therefore, it is reasonable to assume that the dynamics is driven to a scale-invariant attractor that is independent of the initial conditions, as is normal in nonlinear systems.

The power-law form of the galaxy-galaxy correlations can be taken as evidence of scale invariance, although there may be deviations from pure power laws. In particular, Zehavi et al (2004) find small but systematic deviations in the projected correlation function of a sample from the Sloan Digital Sky Survey. They relate those deviations to the deviations from a power-law correlation function found by Jenkins et al (1998) in Λ -CDM simulations. Hence, they interpret them as caused by the transition from a two-halo regime on large scales to a one-halo regime on small scales. We shall discuss an alternative interpretation at the end of this paper, after we have introduced and explained the multifractal model of halos. Our interpretation is fully consistent with scale invariance.

Halo models of large-scale structure are now well developed (Cooray & Sheth, 2002). They assume that the full dark matter distribution is composed of two parts: the dark matter distribution within halos and the distribution of halos themselves. The matter distribution within halos is considered to be in virial equilibrium. This inner distribution has received much attention. Usually, it is assumed to be relatively smooth, and it is useful to define the average “profile” of a single halo. The first approximation is a power-law profile (Peebles, 1974; Sheth & Jain, 1997; Murante et al, 1997). However, more refined profile models involve a crossover between two power laws (Cooray

& Sheth, 2002).

Regarding the distribution of halos, halo centers have been distributed randomly in some models (Peebles, 1974; McClelland & Silk, 1977; Sheth & Jain, 1997; Murante et al, 1997) but clustering in the distribution of halos has also been considered (Mo & White, 1996; Sheth & Tormen, 1999). Clustering of halos is to be expected and, in particular, the clustering of halos can be of fractal type. In fact, a power-law halo profile and a fractal distribution of halos are just two aspects of a new formulation of the multifractal model (Gaite, 2005-A). In this formulation, a general multifractal is considered as a set of fractal distributions of halos, such that similar halos have a fractal distribution with a given dimension.

However, the separation of the full matter distribution between a distribution within halos and a distribution of halos is not meaningful if the full distribution is scale invariant. A power-law profile actually prevents one from assigning definite sizes or masses to halos, which must be associated, in principle, with *point-like* mass singularities (Gaite, 2005-A). But the dark matter distribution is not scale invariant on ever decreasing scales. Thus, the breaking of scale invariance induces a change in the nature of the matter distribution that allows us to assign halos a definite size.

More in general, we will see that the fine structure intrinsic to mathematical multifractals on ever decreasing scales gives rise to some counter-intuitive and even paradoxical geometrical notions. Some of these notions are relevant to describe the dark matter distribution, in spite of its not being scale invariant on ever decreasing scales.

Thus, our definition of halo differs from the usual definition: we understand that a natural definition of halo in a multifractal model with a natural coarse-graining scale assigns halos equal size, namely, the size of that scale. A similar definition, namely, based on a uniform size, was proposed by Vergassola et al (1994) to define a mass function for the structure produced in the adhesion model. In contrast, the most popular definition of halo is based on the *spherical collapse* formalism (Mo & White, 1996; Sheth & Jain, 1997, Cooray & Sheth, 2002), and it assumes that halos are given by a density-contrast threshold ($\delta\rho/\rho = 178$). This definition of halo constitutes the basis for the halo finders that use the “friends-of-friends”

(FoF) technique (Davis et al, 1985). Nevertheless, Valageas, Lacey & Schaeffer (2000) have shown that both choices, namely, halos given by a density condition or equal-size halos, can be considered adequate from a theoretical point of view. Our multifractal model of halos agrees with their conclusion, for its crucial feature is the pattern in which the mass concentrates rather than the division of mass among individual halos, which can be made in various manners. Of course, the simplest manner is to take equal-size halos.

The notion of void as basic element of the large scale structure is now well established, but its definition is more imprecise than the definition of halo. The original definition of void as a totally empty region, suitable for the galaxy distribution, is now being replaced with definitions that allow for partial emptiness, after having been admitted that dark matter and even low luminosity galaxies are present in the initial voids. In fact, recently, Shandarin, Sheth & Sahni (2004) have defined void as an *underdense connected* region, such that voids are complementary to superclusters. We propose here a definition that is related with the definition of Shandarin, Sheth & Sahni (2004), but which hinges on the nonlinear multifractal nature of the distribution, unlike theirs.

We begin with a brief review of of multifractals, focusing on the concept of mass concentrations (singularities) and the realization of scale invariance. We introduce the key concept of multifractal spectrum and, in particular, the bifractal spectrum, as well as the method of calculation of the spectrum from correlation moments. Halos can be identified with singular mass concentrations, with power-law profile, whereas voids can be identified with regular mass depletions. Useful computational notions of halo and void result when we consider a (natural) coarse-graining scale. This leads us to a general study of the coarse-grained probability distribution function and its connection with the lognormal model. Further connection with the Press-Schechter mass function is also possible. Then we study what implications a multifractal model has for the distribution of halos (as we have defined them). Finally, we test all these notions against cosmological N -body simulations.

2. Multifractals and mass concentrations

Multifractal measures appear frequently in physics. In particular, they appear frequently as attractors of dynamical systems (Halsey et al, 1986; Falconer, 2003). In dynamical systems, the natural measure of some region represents the portion of time that the system spends in it. For many systems, one indeed finds that, at long times, the trajectory is confined to a small region of the available space (an attractor), but the time that it spends in any subregion of it is very variable. In other words, the measure is very irregular and this non-uniformity encodes further structure that defines the attractor.

The formation of large scale structure is given by the cosmological Newton-Poisson equations (Peebles, 1980), which constitute a dynamical system. Therefore, to justify the relevance of multifractal analysis in the description of large scale structure, we may adopt the natural view that this structure is just an attractor of that many-dimensional dynamical system. Or we may argue that we expect a scale-invariant structure, but in which the realization of scale invariance is non-trivial, as in general multifractals. At any rate, the final justification must rest on a successful comparison with observational data or results of cosmological simulations.

As said above, multifractal measures represent mass distributions spread according to highly irregular patterns, that is, with mass concentrations of very different magnitude (Falconer, 2003). This magnitude is referred to as “strength” and defined by the local dimension α (also called Lipschitz-Hölder exponent in the mathematical literature); namely,

$$\alpha(\mathbf{x}) = \lim_{r \rightarrow 0} \frac{\log m[B(\mathbf{x}, r)]}{\log r}, \quad (1)$$

where $m[B(\mathbf{x}, r)]$ is the mass in the ball of radius r centered on the point \mathbf{x} . We also write, informally, $m[B(\mathbf{x}, r)] \sim r^{\alpha(\mathbf{x})}$. We only consider points \mathbf{x} such that $m[B(\mathbf{x}, r)]$ does not vanish for any $r > 0$, to prevent the divergence of $\alpha(\mathbf{x})$. These points form the *support* of the measure.

In a regular mass distribution, $\alpha = 3$ (constant). So a multifractal is a singular mass distribution and its mass concentrations are also called singularities (of various strengths). On the other

hand, an ordinary self-similar fractal can be considered endowed with a uniform mass distribution over it, such that $\alpha < 3$ is the *constant* fractal (Hausdorff-Besicovitch) dimension. Thus, in the context of multifractals, ordinary self-similar fractals are called *monofractals* (or *unifractals*). Full-fledged multifractals possess a range of exponents α (or strengths), namely, $0 \leq \alpha_{\min} \leq \alpha \leq \alpha_{\max}$. Every set of points in which α takes a definite value is a fractal set (in the sense of having non-trivial fractal dimension). Therefore, a multifractal can be considered as a set of fractals containing the various mass concentrations. The *multifractal spectrum* $f(\alpha)$ is the function that gives the fractal dimension of the set of points with exponent α .

Regarding multifractal spectra, we should mention that there are cases in which α is not strictly constant but which cannot be considered full-fledged multifractals. An example is a finite number of (isolated) concentrations of different strength. This is a regular distribution except for the finite number of singularities. It has interest in cosmology, as the basis of the model of randomly-placed power-law halos (Gaite, 2005-A). The locations of these halos may also be correlated, so that the model actually becomes related to the halo model proposed here, as we shall see.

2.1. Correlation moments and multifractal spectrum

To analyze the structure of multifractals, it is useful to introduce the scale-dependent correlation moments

$$M_q(r) = \int dm(\mathbf{x}) m[B(\mathbf{x}, r)]^{q-1}. \quad (2)$$

M_1 is the total mass, which we normalize to one. With this normalization, a multifractal measure can be interpreted as a probability measure. $M_2(r)$ is the usual *mass-radius* relation or two-point correlation integral (the integral of the two-point correlation function). Larger integer values $q = 3, 4, \dots$ are also employed in the analysis of the large scale matter distribution, but they are increasingly difficult to estimate. In addition, since multifractals are singular non-uniform distributions, integer values of q are not sufficient and we have to consider the full set of moments $M_q(r)$ for $-\infty < q < \infty$. We can then define the function that gives the scaling behaviour of this full set of

moments, namely,

$$\tau(q) = \lim_{r \rightarrow 0} \frac{\log M_q(r)}{\log r}. \quad (3)$$

For well-behaved multifractals, this function determines the multifractal spectrum through a Legendre transform (Falconer, 2003):

$$f(\alpha) = \inf_q [q\alpha - \tau(q)], \quad (4)$$

where \inf_q means the infimum with respect to q . If $\tau(q)$ is differentiable and *convex*, the infimum is given by the vanishing of the derivative with respect to q , so

$$\alpha(q) = \tau'(q).$$

Then, after inverting $\alpha(q)$, one obtains

$$f(\alpha) = q(\alpha)\alpha - \tau[q(\alpha)], \quad (5)$$

which is also convex, namely, $f''(\alpha) < 0$.

It is useful to define the quantity $D(q) = \tau(q)/(q-1)$, which is constant for a monofractal, and, in general, decreases with q . It turns out that the most important values of q are $q = 0, 1$. At $q = 0$, we have $f(\alpha_0) = D(0) = -\tau(0)$. On account that $f'(\alpha_0) = q = 0$, the set of singularities with exponent α_0 has the largest fractal dimension (which often corresponds to the measure's support). The value $q = 1$ gives the *entropy dimension* $D(1)$, for a value of α_1 such that $\alpha_1 = f(\alpha_1) = D(1)$. The corresponding singularity set defines the *measure's concentrate*, that is, the set outside of which the measure vanishes. Note that $f'(\alpha_1) = q(\alpha_1) = 1$ and convexity of $f(\alpha)$ imply $f(\alpha) \leq \alpha$ for any α (with equality at α_1).

For a monofractal, it is sufficient to consider the mass-radius relation $M_2(r)$ and its exponent $\tau(2) = \alpha(q) = D(q)$ for all q . In finite samples from fractals, it is usual to consider the discrete version of the mass-radius relation, namely, the number-radius relation $N(r)$, given by the number of particles in a ball of radius r centered on one particle and averaged over every particle,

In general, the mass-radius relation $M_2(r)$ has exponent $\tau(2) = D(2)$. According to Eq. (5) and the condition $f(\alpha) \leq \alpha$,

$$f(\alpha_2) = 2\alpha_2 - \tau(2) \leq \alpha_2 \Rightarrow f(\alpha_2) \leq \alpha_2 \leq D(2),$$

where $\alpha_2 = \alpha(q = 2)$. We can interpret these relations as follows. The multifractal analysis through moments relies on a basic property: only concentrations with *one* exponent contribute to one q -moment, namely, concentrations with the exponent $\alpha(q)$. Therefore, to the mass-radius relation only contribute concentrations with exponent α_2 . These concentrations are distributed in a fractal of dimension $f(\alpha_2)$. The exponent α_2 is larger than $f(\alpha_2)$ due to the presence of other singularities with different α in its neighbourhood. Moreover, since $M_2(r)$ is obtained by averaging over points, this operation further increases the exponent.

2.1.1. Coarse analysis and counts-in-cells

The mathematical definition of q -moments provided by the integral in Eq. (2) may not be convenient for calculations. Therefore, in analogy with the *box-counting* method for fractal sets, there is a method for *coarse multifractal analysis* (Falconer, 2003): one puts an ℓ -mesh of cubes in the total volume (which is itself a large cube) and considers the mass inside each cube. Then one defines

$$M_q(\ell) = \sum_i m_i^q, \quad (6)$$

where the sum is over non-empty cubes. This method is related to the coarse-graining method used in cosmology for finite samples under the name of “counts-in-cells” (Balian & Schaeffer, 1989-A): assuming that all the particles have the same mass, the mass is measured by counting particles. In coarse multifractal analysis, the linear cube size ℓ defines a scale that one lets go to zero, eventually. In particular, one lets $\ell \rightarrow 0$ to define the function $\tau(q)$ according to Eq. (3) after replacing r with ℓ . From a mathematical standpoint, the equivalence of both point-centered results, from Eq. (2), and lattice-based results, from Eq. (6), is not guaranteed and requires a careful analysis (Falconer, 2003; Harte, 2001).

Since every set of points in which α takes a definite value is a fractal with dimension $f(\alpha)$, in coarse multifractal analysis, the number of cells with exponent α is given by

$$N(\alpha) \sim \ell^{-f(\alpha)}, \quad (7)$$

according to the box-counting interpretation of the dimension $f(\alpha)$. Let us mention the alternate de-

scription provided by its number-radius relation

$$N(\alpha, r) \sim r^{f(\alpha)},$$

namely, the average number of cells with exponent α in a ball of radius $r \gg \ell$ centered on one cell. Note that the opposite sign of the exponent in these two numbers is in accord with their being related to M_0 and M_2 , respectively, and the equality $\tau(2) = D(0) = -\tau(0)$ for a monofractal.

From relation (7), we can obtain the *mass function* at scale ℓ , namely, the number of cells with mass between m and $m + dm$, which is

$$N(m) dm \sim -\ell^{-f(\alpha)} d\alpha.$$

Given that $\alpha \sim \log m / \log \ell$,

$$N(m) \sim \ell^{-f(\alpha)-\alpha}. \quad (8)$$

Any measurement of positions of objects (galaxies, etc.) has to be made with a given precision, which actually defines the *natural* cell size for the corresponding observation. Furthermore, a single object at the given resolution may appear as a compound object at a higher resolution. Therefore, coarse multifractal analysis is naturally adapted to this idea of change in the description of a distribution in terms of single objects as the resolution increases. However, let us note that other coarse-graining procedures and, in general, other methods can be employed for multifractal analysis. In particular, let us point out that Halsey et al (1986) define multifractal analysis by coarse-graining into *arbitrary* (disjoint) pieces S_1, \dots, S_N , such that their diameters fulfill $\ell_i \leq \ell$. Then, the function

$$M_q(\tau, \{S_i\}, \ell) = \sum_{i=1}^N \frac{m_i^q}{\ell_i^\tau},$$

for small ℓ (large N) and optimized over $\{S_i\}$, is of order unity only for some value of τ , for given q . In the case of partitioning into an ℓ -mesh of cubes, this definition of $\tau(q)$ coincides with the value given by Eq. (6).

2.2. Linear multifractal spectrum: bifractals

The *Legendre spectrum* given by Eq. (4) is only an upper bound to the real multifractal spectrum

(Falconer, 2003). Nevertheless, for “reasonable” multifractals they coincide. However, there is an interesting situation in which there can be a discrepancy, as has been noted by Balian and Schaeffer (1989-B). In general, the Legendre spectrum (4) must be *convex* (from above), but the real multifractal spectrum needs not be convex. So the Legendre spectrum associated to a non-convex multifractal spectrum is only its *convex hull*.

For example, let us consider a bifractal, with two exponents α_1 and α_2 (Balian and Schaeffer, 1989-B). We assume that $\alpha_1 < \alpha_2$. Although the multifractal spectrum seems to consist of just two values, namely, $f(\alpha_1)$ and $f(\alpha_2)$, the Legendre spectrum is a full segment with ends at $(\alpha_1, f(\alpha_1))$ and $(\alpha_2, f(\alpha_2))$, that is, a linear spectrum. The corresponding slope of $\tau(q)$ has a jump from α_1 to α_2 at

$$q_* = \frac{f(\alpha_2) - f(\alpha_1)}{\alpha_2 - \alpha_1}.$$

Now imagine that we superimpose on this bifractal another bifractal, either $\{\alpha_1, \alpha_3\}$ or $\{\alpha_3, \alpha_2\}$, such that the exponent α_3 fulfills $\alpha_1 < \alpha_3 < \alpha_2$ and its corresponding dimension fulfills

$$f(\alpha_3) < \frac{f(\alpha_2) - f(\alpha_1)}{\alpha_2 - \alpha_1}(\alpha_3 - \alpha_1) + f(\alpha_1);$$

namely, such that the point $(\alpha_3, f(\alpha_3))$ is below the segment with ends at $(\alpha_1, f(\alpha_1))$ and $(\alpha_2, f(\alpha_2))$. This second bifractal will be *invisible* in both the function $\tau(q)$ (which gives the moments) and the Legendre spectrum.

We can consider a linear multifractal spectrum, with $f''(\alpha) = 0$, as a limit of general convex spectra, with $f''(\alpha) < 0$. To be more precise, if we are given two exponents α_1 and α_2 , and their respective dimensions $f(\alpha_1)$ and $f(\alpha_2)$, convexity implies that $f(\alpha)$, for $\alpha_1 < \alpha < \alpha_2$, lies above the segment with ends at $f(\alpha_1)$ and $f(\alpha_2)$. Assuming that $\tau(q)$ is differentiable, $\tau'(q) = \alpha$ is an decreasing function that interpolates from α_2 to α_1 in a range $[q_1, q_2]$. As $q_1 \rightarrow q_2$, $\tau'(q)$ becomes discontinuous and $\tau(q)$ has an angle, at some value $q_* \in [q_1, q_2]$. Then $f(\alpha)$ collapses to the linear spectrum (from above). In this limit, the multifractal becomes dominated by the two fractals at the ends of the segment, with dimensions $f(\alpha_1)$ and $f(\alpha_2)$. In other words, this is a *bifractal limit* of the multifractal spectrum.

We can distinguish two cases, according to whether q_* is larger or smaller than one. In the former case, the measure’s concentrate fulfills $\tau'(1) = \alpha_2 > \alpha_1$, so $\alpha_2 = f(\alpha_2)$; in the latter case, the measure’s concentrate fulfills $\tau'(1) = \alpha_1$, so $\alpha_1 = f(\alpha_1)$. In words, we distinguish whether the measure concentrates in either the less or the more singular fractal set. In the former case, the measure’s concentrate and support coincide, whereas in the latter case, the measure’s concentrate corresponds to α_1 and the measure’s support to α_2 . Of course, we can also consider the borderline case with $q_* = 1$. In this case, $\alpha = f(\alpha)$ for $\alpha_1 \leq \alpha \leq \alpha_2$, so the measure concentrates uniformly over the full interval.

Let us mention three interesting examples of linear multifractal spectrum, corresponding to the three above-mentioned cases. The first example is a random distribution of a *finite* number of power-law mass concentrations with exponent $\alpha < 3$ (*one* concentration suffices). This is a bifractal with exponents α and 3, and dimensions $f(\alpha) = 0$ and $f(3) = 3$, respectively (Gaite, 2005-A). Of course, the measure concentrates in the regular component. The second example is provided by the one-dimensional adhesion model. Reasoning about the properties of *devil’s staircases*, She, Aurell & Frisch (1992) and Aurell et al (1997) show that the mass distribution produced by that model is bifractal: it has singularities of *delta-function* type, that is, with $\alpha = f(\alpha) = 0$, and there appears, in addition, a component with $\alpha > 1$ and $f(\alpha) = 1$ (homogeneously distributed, in one dimension). The extension of these results to higher dimension is a moot point (Vergassola et al, 1994). The third example corresponds to the borderline type bifractal: it is a bifractal formed by the union of two separate monofractals (with different dimension). In it, the measure is uniformly concentrated, such that each fractal holds a finite fraction of the total mass.

Let us finally note that any piece of a convex multifractal spectrum that is not very curved can be approximated by a linear spectrum and, therefore, by the corresponding bifractal limit. This property will be useful for the connection with the Press-Schechter formalism (Sect. 3.2).

2.3. Halos as mass concentrations

Halo models of large-scale structure assume that the dark matter is in the form of collapsed halos with definite density profile. This profile is established by averaging over angular directions, hence obtaining a radial profile, whose functional form is essentially the same for every halo (but with different parameters). Several forms have been proposed, the simplest one being a power law $\rho(r) \propto r^{-\beta}$, which is also a limit of other more complicated profiles. A power law halo profile can be related with a power law correlation function (Peebles, 1974; McClelland & Silk, 1977; Sheth & Jain, 1997; Murante et al, 1997). It is also intrinsically associated with self-gravity: the Newton-Poisson equations are scale invariant; so we expect that the mass concentrations produced by them are also scale invariant. This argument is valid in the *strongly nonlinear* regime, where the dynamics dominates over the initial conditions. In particular, the *stable clustering* model (Peebles, 1980) supports this hypothesis (Sheth & Jain, 1997).

Therefore, we define halos to have a power-law profile, namely, the *singular* profile $\rho(r) \propto r^{-\beta}$ with $\beta = 3 - \alpha > 0$. But it is obvious that we cannot assign a definite size to a halo with this profile. Indeed, in a multifractal that is scale invariant on ever decreasing scales, as the definition requires, it is not possible to assign a size or a mass to any structure, because that would break scale invariance: any structure must be repeated in every size, reaching up to the homogeneity scale, which is the only existent scale. In consequence, mass concentrations are point-like mass singularities and they can *only* be classified by their singularity strength, given by the exponent α . However, a singular power-law profile cannot be physically realized. In fact, what is available is a *finite* sample from a multifractal, which is not scale invariant on ever decreasing scales.

Thus, on small scales, there is a change in the nature of the matter distribution, related to the breaking of scale invariance, which allows us to assign halos definite size and masses. This change takes place in the large scale distribution of matter and, more clearly, in cosmological N -body simulations, as we shall explain. Of course, on scales smaller than the scale of this change, the power-law halo profile is altered. Its shape may turn

out to fit a different power law, thus becoming a combination of two power laws, like in current halo profile models (Cooray & Sheth, 2002). If we use coarse multifractal analysis, the breaking of scale invariance appears below a given cell size, which we choose as the size of coarse-grained halos. Then, the number of (coarse-grained) halos is finite. In addition to the full set of halos, with their respective masses, the matter distribution is defined by the distribution of their positions. We will treat the distributions of halos in greater detail in Sect. 4.

Let us note that a uniform coarse-graining length is convenient but not mandatory: in multifractal analysis, one can actually choose pieces of very different size, as commented in Sect. 2.1.1. In particular, halos can be defined to have different size and can be given by a different condition. In principle, halos can be defined by a condition on the density, as in the usual definition. The possibility of using various definitions has already been noted by Valageas, Lacey & Schaeffer (2000). We choose a uniform coarse-graining length, following Vergassola et al (1994). It is a convenient choice, well adapted to N -body simulations.

2.4. Voids as mass depletions

We define a void as a region with very low or vanishing density, but we need to make precise what this condition means. The multifractal formalism is very useful in this regard. In this formalism, the singular concentrations to which we associate halos have a power law profile $\rho(r) \propto r^{-\beta}$, with $\beta = 3 - \alpha > 0$. But, if $\alpha \geq 3$, there is no singularity. The value $\alpha = 3$ ($\beta = 0$) is a reference: a mass concentration with this exponent is not really a concentration: its density is regular, namely, non-divergent and non-vanishing. Exponents $\alpha > 3$ correspond to points of vanishing density, which we naturally associate with voids. Furthermore, the total mass in voids vanishes, since the measure's concentrate, with $f(\alpha) = \alpha$, can only be in regions with $\alpha \leq 3$ (note that, necessarily, $f(\alpha) \leq 3$).

However, any neighbourhood of points in voids, with $\alpha > 3$, is not totally empty. It is possible to have mass around points with vanishing density. There may or may not be totally empty voids, according to whether the measure's support occupies the full volume or not: if it does not, there are re-

gions with non-vanishing volume and no mass in them (in mathematical terminology, these regions are *open sets*). If the dimension of the support of the measure is smaller than three, there need to be totally empty voids, and the multifractal is called *lacunar*. In particular, there may be a scaling set of totally empty voids. This is always the case in one dimension if the the measure’s support has dimension smaller than one, but the geometry of voids is more complex in higher dimensions (Gaite, 2005-B; Gaite, 2006).

To illustrate the nature of multifractal voids in a simple case, let us consider again the one-dimensional adhesion model. In this model, the mass is concentrated in *shocks* and their locations form a *dense* set (She, Aurell & Frisch, 1992; Vergassola et al, 1994). The adjective “dense” is understood with its mathematical meaning: a set is dense in an interval, say, if in any sub-interval, however small, there are points of the set; a typical example is the set of rational numbers between 0 and 1. In the one-dimensional adhesion model, while the density at non-shock points vanishes (they have $\alpha > 1$), these points are surrounded by infinitesimally close small shocks that make the mass in any neighbourhood of them to be non-vanishing. Of course, we could make in that distribution a totally empty void by removing the mass in a sub-interval.

With the preceding definition of void, we can actually consider a multifractal distribution (in three dimensions) as the union of (i) halo clusters, that is, clusters of mass concentrations with $\alpha < 3$, (ii) voids, that is, mass depletions with $\alpha > 3$, and (iii) the boundary between both regions, formed by points with $\alpha = 3$. However, we must beware once more of relying on our geometrical intuition when dealing with multifractals: the set of points with $\alpha = 3$ may not be two-dimensional and so it may not constitute a regular boundary. Indeed, the dimension of this set is $f(\alpha = 3)$, which can well be larger than two. We will see in Sect. 5.3 what this implies for the shape of voids in an example from a cosmological simulation.

Let us now consider a coarse-grained multifractal. The coarse-grained density can be defined to be regular everywhere (with no singularities) and it only vanishes at a point if the mass vanishes in a neighbourhood of it. Therefore, the density only vanishes inside totally empty

voids. Nevertheless, we can still define voids as depleted regions comprising coarse-grained exponents $\alpha_i = \log m_i / \log \ell > 3$ ($\alpha_i \rightarrow \infty$ inside a totally empty void). Note that the boundary of voids is then a coarse-grained version of the above mentioned fractal surface, so it loses small pieces as some singularities get smeared.

Finally, we notice that the presence of voids in the galaxy distribution was a principal motivation for the bifractal model of cosmic structure. Let us quote Balian & Schaeffer (1989-B): “The occurrence of a bifractal behaviour is due to the coexistence at the same scales of clusters and voids”. According to our discussion of the linear multifractal spectra in Sect. 2.2, we can deduce that a bifractal in which the voids define one of the two fractal dimensions must be such that the measure concentrates in the more singular set and, in addition, such that the more regular set has $\alpha_2 > 3$ and is associated with the voids. An interesting one-dimensional example is the adhesion model, according to Sect. 2.2. However, “coexistence at the same scales of clusters and voids” takes place in most multifractals, not only in bifractals.

3. The density probability distribution function

In coarse multifractal analysis, moments are defined by Eq. (6). There is a related way to define statistical moments, namely, by using the density probability distribution function, and this definition has been applied to multifractals (Borgani, 1993; Valageas, 1999). If $P(\rho)$ is the probability of having density ρ , then, its moments are

$$\mu_q = \langle \rho^q \rangle = \int_0^\infty d\rho \rho^q P(\rho). \quad (9)$$

Since in multifractals the density does not exist at singular points, ρ in this definition must be also understood as a *coarse-grained density*. Besides, this definition implies that $\mu_0 = 1$, assuming $P(\rho)$ normalized. In contrast, $M_0 \neq 1$, in general, and it is related with the fractal dimension of the measure’s support. In coarse multifractal analysis, the precise relationship between both definitions of q -moments is

$$\mu_q(\ell) = \langle \rho^q \rangle = \frac{\sum_i \rho_i^q}{\sum_i 1} = \ell^{-3q} \frac{M_q(\ell)}{M_0(\ell)} \sim \ell^{\tau(q) - \tau(0) - 3q}$$

(where the sums are over non-empty cells). For example, $\mu_1(\ell)$ is the average density (within the measure's support) and scales with exponent $-\tau(0) - 3 = D(0) - 3 \leq 0$. If the measure's support has dimension 3, then the average density is ℓ -independent. In this case, it is natural to normalize the density field by dividing it by the average density, so that $\mu_1 = 1$ (Valageas, 1999). If the measure's support is fractal, then the average density diverges as $\ell \rightarrow 0$.

Regarding higher moments $\mu_q(\ell)$, $q > 1$, we have

$$\frac{\mu_q(\ell)}{\langle \rho \rangle^q} \sim \ell^{(q-1)[D(q)-D(0)]}.$$

Given that $D(q)$ is a non-increasing function, this quotient is finite, in the limit $\ell \rightarrow 0$, only for a *uniform* multifractal, namely, a regular distribution or a monofractal (we say that a monofractal is uniform because the exponent α is constant). For a generic multifractal, that quotient diverges.

One can derive other relations between moments. For example,

$$\frac{M_q(\ell)}{M_2(\ell)^{q-1}} \sim \ell^{(q-1)[D(q)-D(2)]}, \quad (10)$$

which diverges for $q > 2$, except in uniform multifractals, namely, monofractals (including regular distributions, with $\alpha = 3$). Thus, this latter relation is useful in the context of *hierarchical models*: a scale-independent quotient M_q/M_2^{q-1} implies $D(q) = D(2)$. In other words, “hierarchical correlation functions imply monofractality of the distribution” (Borgani, 1993). An analogous relation holds for $\mu_q(\ell)$ if $D(0) = 3$.

The probability distribution function (PDF) of the coarse-grained density, $P_\ell(\rho)$, is directly related to the mass function and, therefore, to the coarse multifractal spectrum (Sect. 2.1.1): the number of cells with density ρ is the box-counting approximation to the fractal dimension of the set of mass concentrations with exponent $\alpha = \log m / \log \ell = \log \rho / \log \ell + 3$. The general statement of this relation is best made in the context of probability theory, namely, of the theory of *large deviations*. The relevant concepts in this theory appear naturally when we consider the generalization of the central limit theorem to nonlinear distributions and, hence, we regard the lognormal distribution as a general nonlinear PDF.

3.1. Connection with the lognormal model

As a simple extension of the Gaussian density field in the linear regime, Coles & Jones (1991) proposed that a lognormal field model would be suitable for the nonlinear regime, especially, in the *weakly* nonlinear regime. We shall see that a lognormal density PDF is natural in connection with multifractals.

From a purely statistical point of view, the Gaussian distribution is associated with the central limit theorem and one expects that it appear in many situations where the *sum* of a large number of independent random variables is involved. A nonlinear analogue of this theorem is provided by the *multiplication* of independent random variables, because multiplication of these variables is equivalent to addition of their logarithms. Hence, the lognormal distribution arises as the limit distribution in multiplicative processes. This formulation of the lognormal distribution corresponds to the *large-deviation* formulation of multifractals (Frisch, 1995; Sornette, 2000; Harte, 2001), which is particularly adapted to random cascade processes but has a broader scope. We proceed to introducing a few relevant notions, leaving aside unnecessary details.

We may recall that the central limit theorem considers the limit distribution of the sum of n independent random variables with finite variances (and zero mean). It states that this limit distribution is Gaussian, with variance given by the sum of the variances. In the particular case of n independent identically distributed variables, their sum divided by \sqrt{n} has a Gaussian distribution (with the common variance). However, if we want to take into account unlikely events, that is deviations of magnitude larger than \sqrt{n} , we must consider higher moments than the variance. In particular, if we call X the sum of the n variables, as $n \rightarrow \infty$,

$$P[X \sim nx] \sim e^{n S(x)}.$$

In this formula, x is an “intensive” variable, that is, finite in the limit $n \rightarrow \infty$, and $S(x)$ is an entropy function called the Cramér function. This function can be obtained from the full (common) distribution function of the variables (Frisch, 1995; Sornette, 2000). Its second order expansion at its maximum (assumed unique) gives the Gaussian

approximation that constitutes the central limit theorem.

In multiplicative processes, such as random cascades or fragmentation processes, we also have that a good approximation is given by the two basic moments (mean and variance) of the logarithm of the relevant random variable. Therefore, the lognormal distribution appears as the basic approximation to the distribution of mass concentrations in a multifractal. This has already been noted by Jones, Coles & Martínez (1992). The large-deviation formalism becomes necessary if we need to consider mass concentrations that appear rarely, because of their small or large exponent α with respect to α_0 , the value that maximizes $f(\alpha)$ (assumed unique). In fragmentation cascades, the number n in the hierarchy gives the scale, for example, $\ell_n = 2^{-n}$ for a binary division. The sum variable X represents minus the logarithm of the mass, such that the “intensive” variable is now the exponent $\alpha = \log m / \log \ell_n$. Therefore,

$$P[-\log_2 m \sim n\alpha] \sim e^{nS(\alpha)},$$

and we are to identify $S(\alpha)$ with the multifractal spectrum $f(\alpha)$; namely, $S(\alpha) = f(\alpha) \ln 2$. Thus the large-deviation condition is equivalent to focusing on mass concentrations with exponents α such that their supporting regions have small dimension $f(\alpha)$ compared with its largest value. In the “small-deviation” regime, we can use the second order expansion (parabolic approximation) of $f(\alpha)$ at α_0 , the value that maximizes it (assumed unique). This value corresponds to the measure’s support. The “small-deviation” regime is indeed the weakly nonlinear regime, and it gives a lognormal PDF.

Note that Jones, Coles & Martínez (1992) chose to take a parabolic approximation to $f(\alpha)$ that is not its second order expansion but instead makes it tangent to the diagonal, like the full $f(\alpha)$. This choice does not seem related to the theory of large deviations. However, a large-deviation expansion around the measure’s concentrate (the point of tangency to the diagonal) is possible as well. Let us consider the mass moment M_1 and its associated mass PDF

$$m P[-\log_2 m \sim n\alpha] \sim m e^{nS(\alpha)} \sim e^{n[f(\alpha) - \alpha] \ln 2}.$$

In the limit $n \rightarrow \infty$, this density vanishes unless $f(\alpha) = \alpha$, that is, unless in the measure’s con-

centrate. In other words, there is no mass outside the concentrate of the measure (mass), according with its name. Nevertheless, we can consider again a “small-deviation” regime given by the second order expansion around the measure’s concentrate, such that it gives a lognormal mass PDF. Note that this lognormal mass PDF is generally different from the previous lognormal PDF.

We must mention that the lognormal approximation to multifractals assumes that the multifractal spectrum $f(\alpha)$ is well behaved, namely, that it has second derivative. Of course, this condition of differentiability may not hold in some cases. In particular, a bifractal spectrum does not have well-defined second derivative at its maximum.

It is well known that the lognormal distribution is not determined by its moments μ_n , $n = 1, 2, \dots$, that is, there are other distributions with the same set of moments. In physical terms, the reason for this non-uniqueness can be ascribed to the fact that high-order moments are dominated by high-density regions, so that the full set of moments contains insufficient information about very low-density regions or *voids* (Coles & Jones, 1991). This was the motivation for considering the additional information on voids, namely, the void probability function, as a necessary ingredient. In fact, the combination of separate information on clusters and voids, respectively, and the assumption of scale invariance led Balian & Schaeffer (1989-B) to propose a *bifractal* model of large scale structure. From the preceding discussion about the lognormal model and its relation with multifractals, we can deduce that Coles & Jones’s (1991) and Balian & Schaeffer’s (1989) arguments are related and that we do not need to restrict ourselves to bifractals. Indeed, we have already pointed out that the singular nature of multifractals requires us to use the full set of moments $M_q(r)$, for $-\infty < q < \infty$. In particular, negative values $q < 0$ are typically associated with voids.

We have explained the connection between multifractal and the lognormal model of Coles & Jones (1991) in regard to the density PDF. Further connection in regard to n -point correlation functions, if possible, seems to require additional assumptions. We note, in particular, that there is *no scale invariance* in the lognormal model as a field theory, in spite of the arguments presented by Coles &

Jones (1991) regarding a possible connection with multifractality.

3.2. Connection with the Press-Schechter mass function

The usual mass function in halo models is the one given by the Press-Schechter spherical collapse formalism (Mo & White, 1996; Sheth & Jain, 1997). This formalism relies on an initial Gaussian PDF. Regarding the relation that we have established in multifractals between the mass function of halos and the coarse density PDF (for $\alpha < 3$), we shall explore if there is a connection with the Press-Schechter mass function. Let us briefly recall the relevant elements of this formalism.

Let us consider the coarse density and its PDF. For early times or large values of the coarse-graining length ℓ , we can consider the density constant ($\rho = 1$, if the total volume and mass are normalized) except for small fluctuations given by a Gaussian PDF. This Gaussian PDF has a scale-dependent variance $\sigma^2(\ell) \ll 1$. To obtain the mass function of collapsed objects, one needs a criterion to decide which regions of size ℓ will collapse. The simplest criterion is that every region in which the density exceeds some threshold ρ_c must collapse. Given that the PDF is Gaussian, the cumulative distribution function is

$$\begin{aligned} P(\rho > \rho_c) &= \frac{1}{\sqrt{2\pi}\sigma} \int_{\rho_c}^{\infty} \exp\left(-\frac{(\rho-1)^2}{2\sigma^2}\right) d\rho \\ &= \frac{1}{2} \left[1 - \operatorname{erf}\left(\frac{\rho_c-1}{\sqrt{2}\sigma}\right) \right]. \end{aligned} \quad (11)$$

The mass of regions of size ℓ is $m \sim \ell^3$. Therefore, we can express $\sigma^2(\ell)$ in Eq. (11) in terms of the mass of collapsed objects, provided that this equation gives the fraction of regions of mass greater than m that collapse for a given threshold ρ_c . We may call this fraction $F_>(m)$. It is a function of the ratio $(\rho_c - 1)/\sigma$, so that raising the threshold ρ_c at fixed σ is equivalent to diminishing $\sigma(\ell)$ at fixed ρ_c and making density peaks smaller. $\sigma(\ell)$ must be a decreasing function of ℓ and, therefore, of m . Thus, collapse of large masses is suppressed.

The mass function is

$$\begin{aligned} N(m) &= -\frac{dF_>(m)}{dm} \frac{1}{m} = -\frac{1}{m} \frac{dF_>(m)}{d\sigma} \frac{d\sigma}{dm} \\ &= \frac{1}{\sqrt{2\pi}} \frac{1}{m} \frac{d\sigma}{dm} \frac{\rho_c-1}{\sigma^2} \exp\left(-\frac{(\rho_c-1)^2}{2\sigma^2}\right), \end{aligned} \quad (12)$$

where we have introduced the factor $m^{-1} = \ell^{-3}$ which represents the total number of collapsed objects. We assume an initial power-law spectrum of Gaussian fluctuations, namely, $\sigma^2(\ell) \propto \ell^{-n-3}$ ($n > -3$ is the spectral index in Fourier space). Then, the mass function is also a power law, but with an exponential decay for large masses; namely,

$$N(m) \propto \left(\frac{m}{m_*}\right)^{n/6-3/2} \exp\left[-\left(\frac{m}{m_*}\right)^{n/3+1}\right], \quad (13)$$

where m_* stands for the large-mass cutoff.

We must now consider carefully the limitations of the Press-Schechter formalism. For this, we must distinguish the one-dimensional case from the others, including the physical three-dimensional case. The essential assumptions are the validity of an initial Gaussian PDF and of the spherical collapse model. A Gaussian PDF is valid if ℓ is large, namely, $\sigma^2(\ell) \ll 1$. The spherical collapse model amounts to assuming that every overdensity above the threshold gives rise to a symmetric collapsed object. This is a reasonable assumption in one dimension, but it is questionable in higher dimensions. In fact, only a small percentage of the initial overdensities undergo nearly spherical collapse, and they are precisely the largest overdensities (Audit, Teyssier & Alimi, 1997; Lee & Shandarin, 1998). This is particularly clear in the Zeldovich approximation. Thus, the Press-Schechter formalism can only apply, in three dimensions, to the formation of the strongest concentrations (as already noted by Vergassola et al (1994) in their comparison of the Press-Schechter formalism with the adhesion model). The Press-Schechter formalism has been extended to ellipsoidal collapse, with the consequent improvement (Sheth & Tormen, 1999). However, this extension still excludes irregular collapses, which are common for weak concentrations.

In conclusion, the Press-Schechter formalism produces a power-law mass function with a large-mass cutoff, but it can only be applied to massive halos. Considering this formalism as an approximation to the full nonlinear halo mass function based on the linear theory, we would like to explore its relationship with a lognormal PDF, which is valid in the weakly nonlinear regime. Then the question is if relatively strong mass concentrations

can in fact have a power-law mass function (neglecting the exponential cutoff) that is consistent with an overall lognormal-like distribution.

To answer this question, let us mention firstly that it is known that the lognormal distribution can be mistaken for a power law over a relatively large interval (Sornette, 2000, page 80).¹ As a parabolic approximation to a multifractal spectrum, the lognormal distribution derives from the second order expansion around its maximum, representing the measure's support. But the measure's concentrate is best represented by the second order (parabolic) approximation around the point $f(\alpha) = \alpha$, as explained in Sect. 3.1. This second parabola can actually be very close to the first one. In any event, an even simpler approximation is the first order (linear) approximation around the point $f(\alpha) = \alpha$.

In fact, a poor sampling of a multifractal will mainly reflect the measure's concentrate. Let $\alpha_1 = \alpha(1)$; given that $\alpha_1 = f(\alpha_1)$ and $f'(\alpha_1) = 1$, the linear approximation around the measure's concentrate has unit slope, such that it becomes an even bifractal (not loaded toward either the more or the less singular end, as explained in Sect. 2.2). In contrast, note that the power-law part of the Press-Schechter mass function, Eq. (13), produces a divergence in its integral over m in the limit $m \rightarrow \infty$. Of course, this divergence is killed by the exponential factor. Nevertheless, it indicates that *the mass concentrates on massive halos*. In this regard, the Press-Schechter mass function is analogous to the mass function of the one-dimensional adhesion model (according to our discussion in Sect. 2.2). This is not surprising: the one-dimensional adhesion model is the simplest mathematical description of the notion of collapse of overdensities, realizing a collapse into delta-type singularities (Vergassola et al, 1994).

4. The fractal distribution of halos

The realization of scale invariance in a multifractal is characterized by the multifractal spec-

trum. In Sect. 2.1.1, we have shown its relation to the mass function, which is related in turn to the PDF $P_\ell(\rho)$. This PDF can be represented by the statistical moments $\mu_q(\ell)$ (Sect. 3). However, in cosmology, it is normal to measure correlations of a given class of objects rather than moments of the total dark matter distribution. More precisely, one measures positions of luminous objects, namely, galaxies, and computes their correlation functions to establish the statistical properties of the distribution, which may include scale invariance, etc. One can associate galaxies with dark matter halos and, therefore, deduce statistical properties of the distribution of these halos; and viceversa. This is why the distribution of halos has special interest.

If the full dark matter distribution is scale invariant, then the correlation functions of the distribution of halos must be power laws. More precisely, in a multifractal distribution, every population formed by similar halos is a monofractal, although different populations have different dimensions (Gaite, 2005-A). We can describe this difference between populations as a kind of *bias*, albeit of *non-linear* type.

Actually, the very definition of multifractal implies its interpretation as a set of fractal distributions of mass concentrations (and depletions), classified according to the different values of the exponent α : a set of concentrations with exponent α forms a monofractal of dimension $f(\alpha)$. However, for a given exponent α_* , the corresponding set of concentrations generally has dimension $f(\alpha_*) < \alpha_*$, whereas a monofractal fulfills the equality $\alpha_* = f(\alpha_*)$. This happens because in the neighbourhood of the concentrations with $\alpha = f(\alpha_*)$ are present other concentrations with $\alpha \neq f(\alpha_*)$, the mass of which raises the singularity exponent from $f(\alpha_*)$ to α_* .

In the coarse-grained formulation with fixed halo size ℓ_h , we have a finite number of individual halos which we can classify by their masses. Then, each class defines a population and we can compute its number-radius relation, $N(\alpha, r)$, $\alpha \sim \log m / \log \ell_h$ (Sect. 2.1.1). The fractal dimension obtained from each number-radius relation is the only quantity necessary to determine the corresponding monofractal scaling. Thus, the full set of dimensions obtained in this way constitutes an approximation to the multifractal spectrum (in the range $\alpha < 3$).

¹This fact has also been noted in the astrophysical literature, in a small-scale process: star formation from cloud fragmentation. The theory of Zinnecker (1984) leads to a lognormal mass function, as mentioned by Coles & Jones (1991). Zinnecker (1984) compares the lognormal mass function with Salpeter's power law.

We have defined halos by relying on coarse multifractal analysis with a given cell size. In contrast, the measure $N(\alpha, r)$ is point-centered, like the mass-radius relation, given by Eq. (2) with $q = 2$. However, this combination of lattice and point-centered methods is consistent. Nevertheless, one can also use the coarse-grained probability $P_\ell(\rho)$, providing information on the number of boxes of size ℓ with mass $m \sim \ell^\alpha$ and, hence, on the multifractal spectrum (as explained in Sect. 3.1). Using several values of ℓ , we would reproduce the *histogram method* of calculating the multifractal spectrum (Falconer, 2003), which indeed consists of making histograms of the α_i for several ℓ . This method is, in general, less suitable than the method of moments (which uses the $M_q(\ell)$ of Eq. (6)). In fact, we have found most convenient the procedure that consists of (i) the definition of halo populations at given ℓ_h , and (ii) the calculation of their respective number-radius relations $N(\alpha, r)$. The explanation lies on the effect on correlations of a limited scaling range, as we show next.

4.1. The scaling of correlation moments

In general, the mass distribution can be described by either the coarse-grained probability $P_\ell(\rho)$ or the moments $M_q(r)$ (or $\mu_q(\ell)$). In particular, its multifractal properties can be described by either $f(\alpha)$ or $\tau(q)$, which are related by the Legendre transform (Sect. 2.1) and provide identical information, *in principle*. The formulation of a multifractal as a fractal distribution of halos emphasizes the scale invariance of each halo population; in particular, the number-radius relation $N(\alpha, r)$ expresses the scaling properties of each halo population as a monofractal, such that the full set of exponents of all populations constitutes an approximation to the multifractal spectrum (in the range $\alpha < 3$). Therefore, the full set of exponents also provides an approximation to $\tau(q)$, in the corresponding range of q .

The full mass-radius relation $M_2(r)$ is directly related with the reduced two point-correlation $\xi(r)$, such that scale invariance implies that they both are power laws. Unfortunately, the analysis of the two-point correlation function in cosmological N -body simulations by the Virgo Consortium has not shown any convincing scaling (Jenkins et al, 1998). We do not consider this negative result

as ruling out scale invariance. In fact, we can understand it as an effect of a limited scaling range in a distribution that is actually multifractal, rather than monofractal. Let us explain how that effect arises.

The equivalence between $f(\alpha)$ and $\tau(q)$ relies on the one-to-one dependence $\alpha(q)$. However, this one-to-one dependence only holds in a mathematical multifractal (in the limit of ever decreasing scales). In the coarse-grained formulation, we can easily deduce that the average over populations implied by the definition of $M_q(r)$, Eq. (2), will spoil the scaling of *each* particular population (with a given exponent α). In other words, in the coarse-grained formulation, every halo population contributes to some extent to a q -moment (in particular, to $M_2(r)$), rather than only the population with $\alpha(q)$. For this reason, to realize scale invariance, it is preferable to analyse the fractal distributions of halos *independently*, rather than the q -moments of the total distribution.

4.2. The transition to homogeneity

So far, we have used the definitions of scaling exponents, for example, Eq. (1), as implying naive scaling relations, such as $m \sim r^\alpha$. Of course, this relation holds in a limited range of scales (namely, of $\log r$). In addition to the restriction of scaling on small scales, already studied, there has to be a transition to homogeneity on large scales. Over the scale of this transition, say r_0 , the relation $m \sim r^\alpha$ undergoes a crossover to $m \sim r^3$ (homogeneity). Therefore, we can define r_0 by the equation

$$m = \frac{4\pi\bar{\rho}}{3} r_0^3 \left(\frac{r}{r_0} \right)^\alpha, \quad r \ll r_0, \quad (14)$$

where $\bar{\rho}$ is the large-scale mean density. Analogously, the halo number-radius relation $N(\alpha, r) \sim r^{f(\alpha)}$ (Sect. 2.1.1) can also be written as

$$N(\alpha, r) = \frac{4\pi\bar{n}(\alpha)}{3} r_0^3 \left(\frac{r}{r_0} \right)^{f(\alpha)}, \quad r \ll r_0, \quad (15)$$

where $\bar{n}(\alpha)$ is the large-scale mean density of halos of exponent α .

The procedure to determine r_0 from $N(\alpha, r)$ consists of an analysis of the crossover to homogeneity in its log-log graph. It must be done for several values of α , to check that the results

coincide. Actually, the extreme cases are most useful; that is to say, we may take, on the one hand, (a) the smallest value of α (the largest halo mass) such that there is a sufficient number of halos to compute $N(\alpha, r)$, and, on the other hand, (b) the largest value of α (the smallest halo mass) such that its fractal dimension is sufficiently smaller than three as to let us clearly perceive the crossover to homogeneity. In Sect. 5.2, we shall see how to carry out this procedure in an example.

5. Halos and voids in cosmological simulations

In N -body cosmological simulations, the nature of the distribution changes on small scales because there is (i) a minimal mass, corresponding to one particle, and (ii) a softening of the gravitational force. The minimal mass defines the discretization scale, namely, the linear size of the volume per particle. The larger of the discretization scale and the softening scale, usually, the discretization scale, is the natural (intrinsic) coarse-graining scale of the distribution.

Since all the particles have the same mass, the mass is measured by counting particles. We have already defined *coarse multifractal analysis* and mentioned its relation with the method of “counts-in-cells” (Balian & Schaeffer, 1989-A), whereby one puts a ℓ -mesh of cubes in the total volume (which is itself a large cube) and measures the mass inside each cube (cell) by counting particles. In this method, initially and as long as the evolution is linear, cells of the size of the discretization scale contain one particle per cell. Therefore, halos only arise in the nonlinear stage, as they concentrate particles from other regions that become *voids*.

We define mass concentrations (or depletions) at scale ℓ and measure their exponents by the equation $\alpha_i = \log m_i / \log \ell$, where ℓ is the cell size. Standard coarse multifractal analysis proceeds to either (i) make histograms of the α_i for several ℓ (the *histogram method*) or (ii) calculate the moment sums $M_q(\ell)$ in Eq. (6) (Falconer, 2003). Either way leads to an estimation of the multifractal spectrum. However, here we shall combine the “counts-in-cells” method with point-centered methods, according to Sect. 4.

We have applied our numerical methods to sev-

eral N -body cosmological simulations. We present the results of the analysis of the redshift $z = 0$ positions of the Λ CDM GIF2 simulation (by the Virgo Consortium), with 400^3 particles in a volume of $(110 h^{-1} \text{ Mpc})^3$. The force-softening length is $\epsilon = 7 h^{-1} \text{ kpc}$. This simulation is described by Gao et al (2004), who also use it for halo analyses, though they employ the usual FoF definition. Naturally, the discretization length is 400^{-1} (in box-length units) and is considerably larger than the softening length. We determine from it the appropriate halo coarse-graining scale: since we operate with powers of two, we take as halo size $\ell_h = 256^{-1}$. Actually, our results are not very sensitive to the precise value of ℓ_h .

5.1. Counts in cells and halos

In the method of “counts-in-cells”, the qualitative effect of discreteness depends on the cell size, as we study next. If this size is too small, namely, much smaller than the force-softening length, most cells are empty and the non-empty ones have only one particle, so this is the regime totally dominated by the discretization and the gravitational softening. As the size grows, the ratio of non-empty cells grows as well, and some of them begin to have more than one particle. In fact, as the cell size grows, soon a few cells become massive (while the great majority are still empty), in such way that a pattern appears: the number of cells with given mass $N(m)$ becomes a power law. This is shown in Fig. 1.² This regime is still dominated by the discretization.

As the cell size grows larger, at some point, the most numerous cells are no longer the ones with $m = 1$ (Fig. 1). Further increase of the coarse-graining scale eventually leads us to a lognormal-like distribution. We note that this last transition, namely, from the power-law regime to the lognormal-like regime, takes place at a coarse-graining length approximately equal to $\ell_h = 256^{-1}$ (Fig. 1). Thus, this is the scale at which we have

²The power-law dependence of $N(m)$ implies, in particular, that the cumulative cell number $N_{>}(m)$ (the number of cells with mass larger than m) also follows a power law. Since $N_{>}(m)$ is the rank, we have that the rank-ordering of cells follows a power law, that is, it satisfies Zipf’s law (Zipf, 1949; Sornette, 2000). This property also applies to halos, according to our definition. The connection of the Zipf law for voids with fractality has been studied by Gaite & Manrubia (2002) and Gaite (2005-B, 2006).

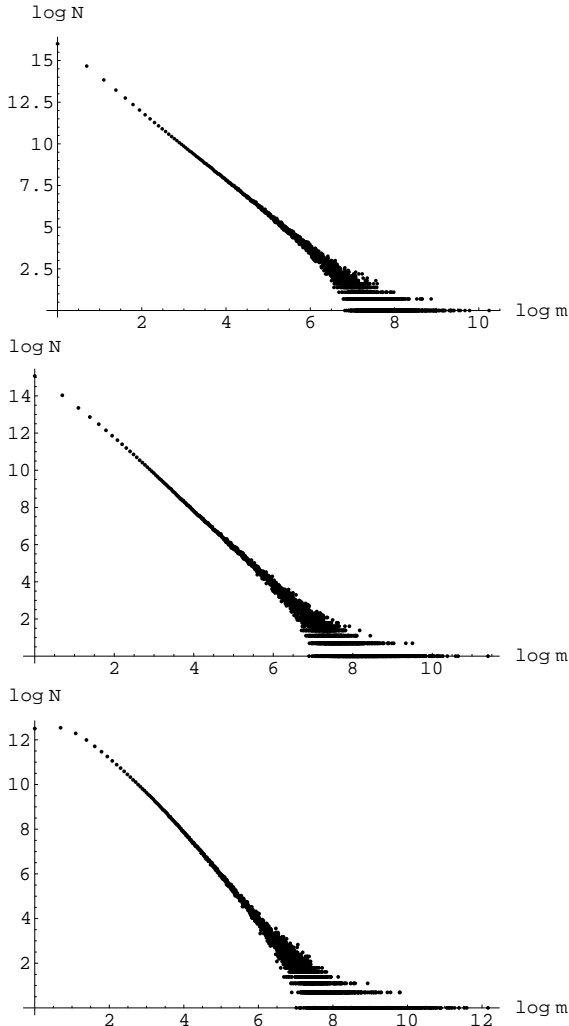


Fig. 1.— Log-log plots of number of halos N versus their mass m (number of particles) at coarse-graining scales 512^{-1} (top), 256^{-1} (middle), and 128^{-1} (bottom). Both the top and middle plots are linear, but the latter, corresponding to lower resolution, already shows a slight decay in the number of light halos. The bottom plot clearly shows a maximum for $m = 2$.

maximal richness and variety of halos, that is, they span the maximal mass-scale range. On the contrary, at this scale, voids are hardly sampled.

Within the power-law regime of $N(m)$, the power law holds very clearly. For example, in the top plot in Fig. 1, in the horizontal axis ($\log m$), the scaling holds from 0 to 7, that is, from $m = 1$ to $m = e^7 = 1097$, namely, three decades (and larger range on the vertical axis). We have performed least-squares fits of $\log N$ versus $\log m$ to find the power-law exponents. To minimize the standard error of the fits, it is convenient to reduce the scaling range. The fit corresponding to $\ell = 256^{-1}$ in the range $m \in [10, 100]$ yields -1.996 ± 0.004 ; the fit corresponding to $\ell = 512^{-1}$ yields -2.022 ± 0.004 . We conclude that $N(m) \sim m^{-2}$. This power law amounts to a linear multifractal spectrum, according to Eq. (8). Moreover, it is consistent with $\alpha = \alpha_1$, corresponding to the measure's concentrate (such that $\alpha_1 = f(\alpha_1)$ and $f'(\alpha_1) = 1$).

The counts-in-cells method of computing $N(m)$ for various coarse-graining lengths would allow us to estimate the multifractal spectrum (according to the histogram method). However, the counts-in-cells formalism is especially suited to compute the moment sums, which provide a more accurate estimation. In fact, it is best to replace in Eq. (6) for q -moments the sum over cells with a sum over number of particles:

$$M_q(\ell) = \sum_{m=1}^{\infty} N(m) m^q. \quad (16)$$

This formula is a discrete version of Eq. (9). In a cosmological simulation, the upper limit to m in the sum is, of course, the total number of particles N_{tot} (400^3 in the GIF2 simulation). In addition, we have to introduce a normalization factor to have $M_1 = 1$; namely, we have to divide m by N_{tot} .

We can deduce from Eq. (16) how halos of different mass contribute to q -moments. Since we have found that the halo mass function $N(m) \sim m^{-2}$, q -moment are given by sums of $q-2$ -powers. In these sums, the contribution of each term increases or decreases with m according to whether q is larger or smaller than 2. In particular, every term of $M_2(\ell)$ contributes equally. This blatantly contradicts the assumption that only contribute

to $M_2(\ell)$ singularities with a given exponent (α_2) and, therefore, a given m .

The assumption that only one α contributes, namely, $\alpha(q)$, is crucial for the scaling of moments, as commented in Sect. 4.1. We display in Fig. 2 the log-log plot of $M_2(\ell)$, for $-9 \leq \log_2 \ell \leq -1$, to show the absence of a convincing scaling range. Indeed, to reach full multifractal scaling, we need to be in the lognormal-like regime of the halo mass function $N(m)$. But this regime appears for cell sizes larger than ℓ_h and up to the transition to homogeneity, comprising a scale range that is insufficient for the scaling of q -moments. Therefore, it is natural that no scaling range of the two-point correlation function was found in the analyses of N -body simulations by the Virgo Consortium (Jenkins et al, 1998). In contrast, scaling is found in the distributions of halos, as we show next.

5.2. Fractal distributions of halos

The description of multifractal large-scale structure in terms of fractal distributions of halos has been explained in Sect. 4. In brief, given the halo size, halos are classified by their masses (or by their exponents, which is equivalent). Then we can directly test if each class of halos is a fractal set by calculating its two-point correlation function, or, rather, its number-radius relation.

The study of fractal distributions of equal-mass halos serves two purposes: first, to provide us with a proof of multifractality and, second, to obtain the homogeneity scale. According to Sect. 4.2, to obtain the homogeneity scale, it is convenient to select two halo populations with extreme values of the halo mass (but the light halo population must not be too homogeneous). Actually, we need a range of masses in each population to have a sufficient number of halos to compute the number radius relation. We choose two ranges, with 750 to 1000 particles and with 100 to 150 particles, defining two populations consisting of 2508 and 25556 members, respectively (see Fig. 1, middle plot).

Results of the analysis appear in Fig. 3: on the top, there is a 1/8-thick slice that shows the aspect of both halo populations; below we have log-log plots of the number-radius functions for the respective spatial distributions. They have similar scaling ranges, but corresponding to quite differ-

ent fractal dimensions, namely, 1.1 and 1.9. The scale of transition to homogeneity, according to Eq. (15), is $r_0 \simeq 1/4$. Intermediate mass values (~ 300) yield intermediate dimensions but similar r_0 .

5.3. The structure of voids

In our definition of void, in Sect. 2.4, we outlined how coarse-graining affects the structure of voids. As said above, in N -body simulations, halos only arise in the nonlinear stage, as they concentrate particles from other regions that become *voids*. Moreover, these voids are *totally empty*, because a cell with less than one particle has to be empty. However, an improvement in mass resolution can be achieved with a relatively simple numerical technique: re-simulation of selected regions. Indeed, re-simulation of voids with higher resolution unveils new structure, similar to the structure with the initial resolution (Gottlöber et al, 2003). This new structure includes small halos. In the words of Gottlöber et al (2003), “the haloes are arranged in a pattern, which looks like a miniature Universe”. This type of self-similar structure corresponds to a multifractal.

In our analysis of the Λ CDM GIF2 simulation, we have taken $\ell_H = 256$, so the smallest halos have about 4 particles and cells with fewer particles belong to voids. We note that the boundary of voids cannot have a good pictorial definition in this situation. To appreciate the complicated geometry of this boundary, we have plotted in Fig. 4 a smoothed version of a two-dimensional section of it (obtained by means of isodensity contours).

The voids displayed in Fig. 4 look quite empty. However, some particles lie in them. Moreover, re-simulation of a region in them with higher resolution (as in Gottlöber et al, 2003) would surely unveil new structure similar to the structure already formed by halo clusters in Fig. 4, but in smaller size. That is to say, many small halo clusters would pop out in the voids. At the same time, if the re-simulation were extended to the roundish small halo clusters already displayed in Fig. 4, they would become less round and more crumpled, like the large ones.

5.4. Multifractal spectrum

Finding fractal distributions of halos with definite scaling exponents constitutes a proof of multifractality. However, we must also apply the standard method of multifractal analysis, namely, the calculation of q -moments and, hence, the multifractal spectrum, according to Eqs. (3) and (5). Since q -moments have no well defined scaling, $\tau(q)$ is not well defined. Nevertheless, it can be computed at any given scale, understanding Eq. (3) as an equation at the given scale rather than a limit. Then, we can study how the multifractal spectrum given by Eqs. (4) and (5) changes across the scales.

Therefore, we have computed the multifractal spectrum from q -moments for various $\ell_n = 2^{-n}$, namely, $\log_2 \ell = -9, \dots, -5$, and plot the results in Fig. 5. We can see that the multifractal spectrum is stable in the range of α where all the curves overlap. For the decreasing part of $f(\alpha)$, which corresponds to negative q , we have only two curves. Their agreement is sufficient for smaller α but they separate for larger α ($\alpha > 4$). This was to be expected, for these values correspond to the most depleted voids, which are not sampled.

The collapse of the $f(\alpha)$ curves along such a considerable range of α and for a considerable range of scales is surprising indeed (compare with the log-log plot of $M_2(\ell)$ in Fig. 2). Furthermore, the stability of $f(\alpha)$ contrasts with the change of the halo mass function from power law to lognormal that takes place over the smaller scales in Fig. 5. In this regard, our conclusion is that the crucial condition in the calculation of the multifractal spectrum by the method of moments has some sort of self-consistency; namely, the condition that only singularities with exponent $\alpha(q)$ contribute to the q -moment (Sect. 4.1), allows one to *extrapolate* the multifractal spectrum to small scales.

Here is a number of consequences that can be directly extracted from the coarse multifractal spectrum, such as is displayed in Fig. 5:

- The entropy dimension is $\simeq 2.5$. This means that this multifractal is concentrated in a set which is not very far from being homogeneous (dimension three).
- The largest fractal dimension is actually three, so this is the dimension of the mea-

sure's support. In conjunction with statistical homogeneity, this essentially means that there are no totally empty voids in the full dark matter distribution (see the comments in Sect. 5.3).

- $\alpha(q = 0) \simeq 3.3 > 3$. This value corresponds again to the multifractal support. We remark that it is formed by mass depletions, that is, such that they belong to voids. Therefore, voids (though *not* totally empty) dominate the distribution (see also Fig. 4).
- The set of regular points with $\alpha = 3$ (non-vanishing density), namely, the boundary of voids, turns out to have $f(\alpha) \simeq 2.9$. This fractal dimension is very close to three. This does not necessarily mean that each piece of surface is very crumpled, because the fractal dimension is also a measure of fragmentation (Mandelbrot, 1977). Therefore, its large dimension surely results from the proliferation of small halo clusters that fill the voids. This type of geometry can be inferred from Fig. 4.

6. Conclusions

We have shown that a statistically self-similar multifractal model explains the relevant features of the geometry of the large scale structure of matter. We have described this multifractal model as consisting of singular mass concentrations and regular mass depletions (plus a boundary between both). Hence, we have proposed to identify mass concentrations with halos and to identify mass depletions as belonging to voids. The identification of halos with mass concentrations implies, in the scale-invariant limit, that they have an *average* power-law profile, although they can actually be very anisotropic. In addition, halos are clustered with a power-law form of its two-point correlation functions. In particular, every population of mass concentrations with equal strength (singularity exponent) has a definite fractal dimension.

We have emphasized that scale invariance, in fact, forbids one to distinguish the mass distributions of matter inside halos from the distribution outside. That is to say, scale invariance actually deprives halos of meaning as entities with a given size (or mass), so they can only be classified by their *strength* exponent. Therefore, halos can only be given a size in connection with the breakdown

of scale invariance. In this connection, the number of halos becomes finite and their average profile changes. In cosmological N -body simulations, we have argued that it is most convenient to use the *uniform* coarse-graining length given by the discretization scale (the linear size of the volume per particle).

The uniform size of halos in our multifractal model can be interpreted in terms of standard coarse multifractal analysis. In N -body simulations, which use equal-mass particles, coarse multifractal analysis becomes equivalent to the method of counts-in-cells. Each halo is formed by a variable number of particles, a number which can be small. Each population of halos with (about) the same number of particles forms a monofractal with a definite dimension. We have analysed, in the Virgo Λ -CDM GIF2 simulation, the mass function of halos and their distribution. The distributions of the different populations of halos show well-defined scaling ranges, corresponding to different scaling dimensions, and shows a common scale of transition to homogeneity. We have selected two representative populations of heavy or light halos, resulting in fractal dimensions $D = 1.1$ or $D = 1.9$, respectively. Note that these two values span the usual range of fractal dimensions measured in the galaxy distribution. The conclusion of our analysis of the GIF2 simulation is that scale invariance holds in the nonlinear regime reproduced in N -body simulations and that it can be measured, contrary to the conclusion of Jenkins et al (1998).

The scale of transition to homogeneity in the fractal distributions of halos of the GIF2 simulation is, in physical units, $r_0 \simeq 14 h^{-1}$ Mpc. Although this value corresponds to a dark-matter simulation, it roughly agrees with standard values found in the galaxy distribution.

The fractal distributions of halos with different dimensions are biased with respect to the full particle distribution, which has fixed mass-radius dimension $D(2)$. Of course, this bias is different from the usual linear bias assumed in cosmology, which only affects the *amplitude* of the two-point correlation function: it is a bias that affects the exponent, that is to say, the fractal dimension. We may properly call this kind of bias *nonlinear bias of scaling type*.

Mass depletions, belonging to voids, are very

undersampled in N -body simulations: by definition, depleted halo-size cells have no particles; or they have a few of them, at the most, if we define the halo size to be somewhat larger than the discretization scale. So the few particles in voids are a gross representation of the small halos that one would find there at a higher resolution. In this regard, our conclusion is similar to that of Kuhlman, Melott & Shandarin (1996). However, self-similarity allows us to draw further conclusions regarding the distribution of matter in voids, since the properties of the distribution can be obtained by coarse multifractal analysis with larger cell sizes.

As to the rôle of correlation moments, multifractals are defined by the full set of moments $M_q(r)$ for $-\infty < q < \infty$ (or the PDF moments $\mu_q(r)$ plus $M_0(r)$), whereas monofractals are defined only by $M_2(r)$. In particular, monofractals fulfill the hierarchical relation $M_q \sim M_2^{q-1}$, for any q . Thus, the singular *and* heterogeneous nature of multifractals implies that the moments with $q = 2, 3, \dots$ are not sufficient. In fact, most important are $q = 0, 1$, associated to the measure's support and concentrate, respectively. Larger q 's are also relevant, in particular, $q = 2$, but the information gathered from large- q moments only applies to the strongest concentrations (most massive halos). The negative- q moments are related to the distribution of matter in voids. Therefore, they are affected by the undersampling of voids. However, if the scaling range is sufficiently large, these negative- q moments can be calculated (approximately), as well as the part of the multifractal spectrum given by them.

Regarding q -moments of the full mass distribution in N -body simulations, we have seen that they scale poorly. In contrast, the analysis in terms of fractal populations of equal-mass halos by their number-radius relation (or two-point correlation function of their positions) provides good scaling, suitable for calculating the fractal dimension of each population. The reason for the poor scaling of q -moments is that the one-to-one correspondence between mass concentrations (or depletions) and q -moments given by the function $\alpha(q)$ is only approximate when the scaling range is limited. If several concentration strengths contribute to the same q -moment, their mixing spoils the scaling of that q -moment. We have discussed in Sect. 5.1

how this mixing of halo populations takes place.

In particular, the various halo populations contribute evenly to M_2 and, hence, to the full two-point correlation, altering its scaling. Therefore, it is natural that Jenkins et al (1998) observed deviations from scaling in their analysis of N -body simulations. It is also natural that Zehavi et al (2004) observe deviations from scaling in their analysis of the Sloan Digital Sky Survey: if one associates galaxies to halos, their distribution is likely multifractal, so the mixing of populations takes place as well. In fact, Zehavi et al (2005) and Tikhonov (2006) have found that the slope γ of the log-log plot of the two-point correlation decreases with luminosity, which agrees with a multifractal distribution.

In the GIF2 simulation, at the scale of the halo size ℓ_h , the mass function is well described by a power law, so that it corresponds to a linear multifractal spectrum and the distribution is actually *bifractal*. To be precise, we find $N(m) \sim m^{-2}$, very accurately. Therefore, the corresponding bifractal fulfills $\alpha = f(\alpha)$ and is an even bifractal, in which the measure is uniformly concentrated (not loaded toward either the more or the less singular end, as explained in Sect. 2.2).

Thus, the bifractal mass function furnished by equal-size halos must be distinguished from the Press-Schechter mass function, which (apart for the large-mass cutoff) is equivalent to a linear multifractal spectrum concentrated on the singular end, that is to say, on the heavy halos. Note that Eq. (13) shows that a mass function $N(m) \sim m^{-2}$ is associated with the spectral index $n = -3$, which is just beyond the allowed range. Of course, equal-size and Press-Schechter halo mass functions were expected to differ. However, it is remarkable that both have a power-law range and that the constant exponent that appears with our definition is a limit case of the Press-Schechter mass function. In any event, we must point out that the exponent -2 for equal-size halos is *independent of the initial power spectrum*, in accord with the nonlinear nature of the multifractal.

The mass function of halos is bifractal (a power law), but the calculation of the multifractal spectrum through moments for cell sizes larger than ℓ_h shows convergence towards a convex, lognormal-like spectrum (Sect. 5.4). We conclude that, at the halo-size scale ℓ_h , the mass discretization does not

allow for a good sampling of halos and allows for almost no sampling of voids. Poorly sampled halos mainly reflect the measure's concentrate. Therefore, the power law is merely a linear approximation to the full mass function near the measure's concentrate. In this regard, let us remark that, in a multifractal that is scale invariant on ever decreasing scales, the *total* mass concentrates in the set such that $\alpha = f(\alpha)$. Paradoxically, mass concentrations with larger α are too few to hold any mass, even all together. On the other hand, mass concentrations with smaller α (or mass depletions) are abundant, but their total mass vanishes nonetheless.

I am grateful to Liang Gao for kindly supplying me with the GIF2 data. My work is supported by the "Ramón y Cajal" program and by grant BFM2002-01014 of the Ministerio de Educación y Ciencia.

REFERENCES

- Audit E., Teyssier R. & Alimi J.-M., 1997, A&A, 325, 439
- Aurell E., Frisch U., Noullez A. and Blank M., 1997, Journ. Stat. Phys. 88, 1151
- Balian R. & Schaeffer R., 1988, ApJ, 335, L43
- Balian R. & Schaeffer R., 1989-A, A&A, 226, 1–29
- Balian R. & Schaeffer R., 1989-B, A&A, 226, 373–414
- Botaccio M., Montuori M. & Pietronero L., 2004, Europhysics Letters, 66, 610
- Borgani S., 1993, MNRAS, 260, 537
- Colombi, S., Bouchet, F.R. and Schaeffer, R., 1992, A&A, 263, 1
- Cooray A. & Sheth R., 2002, Phys. Rep. 372, 1
- Davis M., Efstathiou G., Frenk C. and White S.D.M., 1985, ApJ, 292, 371.
- Domínguez-Tenreiro R. & Martínez V.J., 1989, ApJ 339, L9
- Falconer K., 2003, Fractal geometry — Mathematical Foundations and Applications, Second Edition, John Wiley & Sons, Chichester, UK

- Frisch U., 1995, *Turbulence: The Legacy of A.N. Kolmogorov*, Cambridge University Press.
- Gaite, J., 2005-A, *Europhysics Letters* 71, 332–338
- Gaite, J., 2005-B, *Eur. Phys. Jour. B*, 47, 93
- Gaite, J., 2006, *Physica D* 223, 248
- Gaite, J. and Manrubia S. C., 2002, *MNRAS*, 335, 977
- Gao L., White S.D.M., Jenkins A., Stoehr F. & Springel V., 2004, *MNRAS*, 355, 819
- Gottlöber, S., Lokas, E.L., Klypin, A. & Hoffman, Y., 2003, *MNRAS*, 344, 715
- Halsey T.C., Jensen M.H., Kadanoff L.P., Procaccia I. & Shraiman B.I., 1986, *Physical Review A*, 33, 1141
- Harte D., 2001, *Multifractals: theory and applications*, Chapman & Hall
- Jenkins, A., Frenk, C. S., Pearce, F. R., Thomas, P. A., Colberg, J. M., White, S. D. M., Couchman, H. M. P., Peacock, J. A., Efstathiou, G., and Nelson, A. H., 1998, *ApJ* 499, 20
- Jones B.J., Coles P. and Martínez V., 1992, *MNRAS*, 259, 146
- Jones B.J., Martínez V., Saar E. and Einasto J., 1988, *ApJ*, 332, L1
- Jones B. J., Martínez V. J., Saar E. and Trimble V., 2004, *Rev. Mod. Phys.* 76, 1211
- Kuhlman B., Melott A.L. and Shandarin S.F., 1996, *ApJ*, 470, L41
- Lee J. and Shandarin S.F., 1998, *ApJ*, 500, 14–27
- Mandelbrot B.B., 1977, *The fractal geometry of nature*, W.H. Freeman and Company, NY
- Martínez, V.J., Jones, B.J., Domínguez-Tenreiro, R. & van de Weygaert, R., 1990, *ApJ*, 357, 50
- McClelland J. & Silk J., 1977, *ApJ*, 217, 331
- Mo, H.J. and White, S.D.M., 1996, *MNRAS*, 282, 347
- Murante G., Provenzale A., Spiegel E.A. & Thieberger R., 1997, *MNRAS* 291, 585
- Parisi G. & Frisch U., 1985, On the singularity structure of fully developed turbulence, in *Turbulence and Predictability in Geophysical Fluid Dynamics, Proc. Intnl. School of Physics ‘E. Fermi’, 1983, Varenna (Italy)*, 84–87, eds. M. Ghil, R. Benzi and G. Parisi, North-Holland, Amsterdam
- Peebles P.J.E., 1974, *A&A*, 32, 197
- Peebles, P.J.E., 1980, *The large-scale structure of the universe*, Princeton U. Press, Princeton, NJ
- Pietronero L., 1987, *Physica A* 144, 257–284
- Shandarin S.F., Sheth J.V. and Sahni V., 2004, *MNRAS*, 353, 162
- She Z., Aurell E. and Frisch U., 1992, *Commun. Math. Phys.*, 148, 623
- Sheth, R.K. and Jain, B., 1997, *MNRAS*, 285, 231
- Sheth, R.K. and Tormen, G., 1999, *MNRAS*, 308, 119
- Sornette, D., 2000, *Critical phenomena in natural sciences*, Springer-Verlag
- Sylos Labini F., Montuori M. and Pietronero L., 1998, *Phys. Rept.*, 293, 61
- Tikhonov A., Correlation Properties of Galaxies from the Main Galaxy Sample of the SDSS Survey, preprint [astro-ph/0610643](#)
- Valageas P., 1999, *A&A*, 347, 757
- Valageas P., Lacey C. and Schaeffer R., 2000, *MNRAS*, 311, 234–250
- Valdarnini R., Borgani S. & Provenzale A., 1992, *ApJ*, 394, 422
- Vergassola M., Dubrulle B., Frisch U. & Noullez A., 1994, *A&A* 289
- Yepes G., Domínguez-Tenreiro R. & Couchman, H.P.M., 1992, *ApJ*, 401, 40
- Zehavi I., et al, 2004, *ApJ*, 608, 16
- Zehavi I., et al, 2005, *ApJ*, 630, 1
- Zinnecker H., 1984, *MNRAS*, 210, 43

Zipf G.K., 1949, Human behavior and the principle of least effort, Addison-Wesley Press Inc., Massachusetts

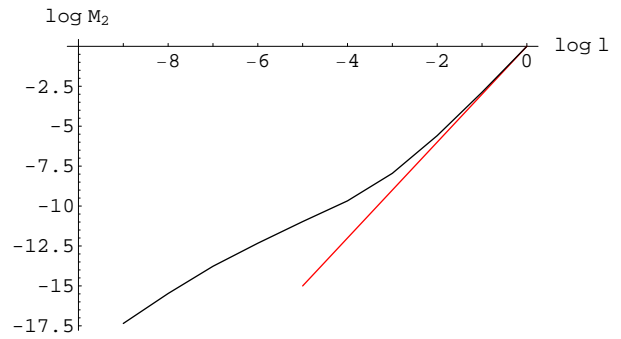


Fig. 2.— Log-log plot of $M_2(\ell)$ (logarithms are to base 2 and the total size is normalized to unity). Note the reduced, hardly noticeable scaling range (the straight line corresponds to homogeneity).

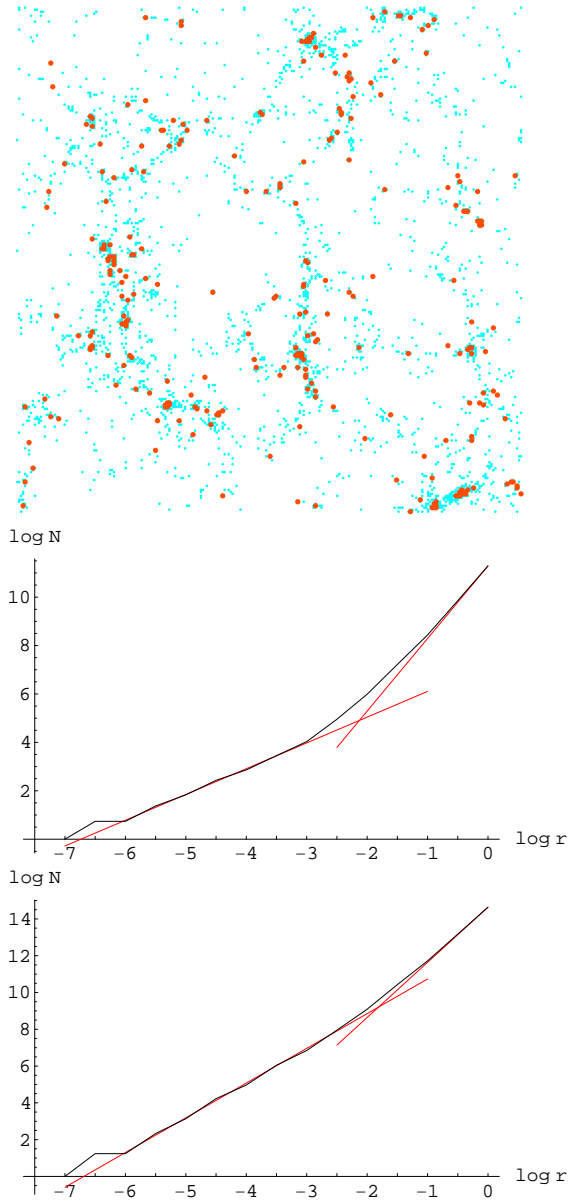


Fig. 3.— Selection of two halo populations from the GIF2 N -body simulation: heavy haloes with 750 to 1000 particles and light haloes with 100 to 150 particles. (Top) 1/8-thick slice showing heavy haloes in red and light haloes in blue. (Down) Number-radius relation for each halo population, showing fractal dimensions 1.1 and 1.9, respectively, and a transition to homogeneity in both (logarithms are to base 2 and the total size is normalized to unity).

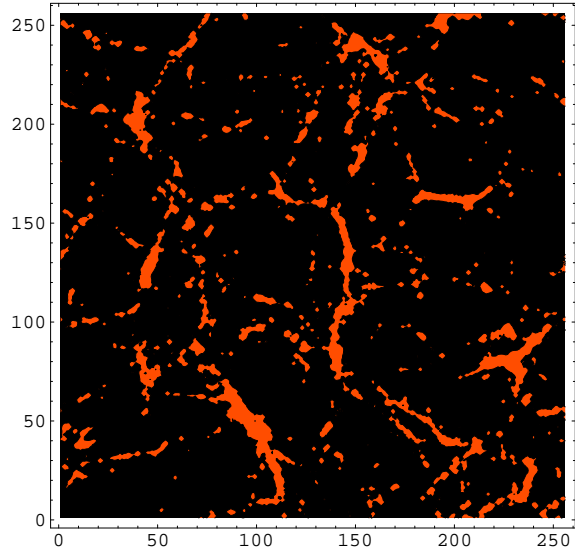


Fig. 4.— A section of the isodensity contour of the smoothed density field at the density corresponding to $\alpha = 3$. The dark area corresponds to mass depletions with $\alpha = 3$ and the light area corresponds to mass concentrations with $\alpha = 3$, namely, to halos. The boundary is a very complex curve, with dimension larger than one.

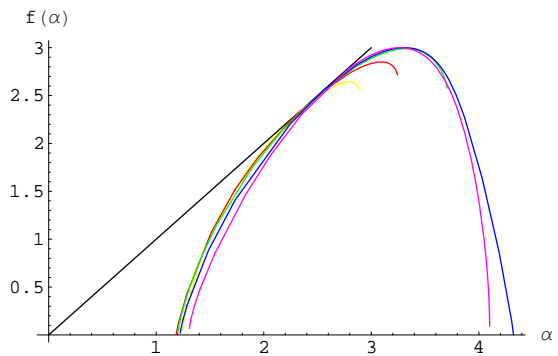


Fig. 5.— Full multifractal spectrum $f(\alpha)$ for $\log_2 \ell = -9, -8, -7, -6, -5$ (yellow, red, green, blue, magenta). We have also plotted the diagonal line to show how the multifractal spectrum is placed under it and touches it at the measure's concentrate dimension $\alpha \approx 2.5$.